

E-144: Proposed Synchrotron Radiation Diagnostic

1 Introduction

Dave Meyerhofer proposes to diagnose the time jitter between the laser and the electron beam using electro-optic switching of infrared synchrotron radiation. In preparation for that measurement we propose to construct a monitor for synchrotron radiation that could be installed in the γ -line of the FFTB downstream of the E-144 IP2, and upstream of Clive Field's backscattered-photon monitor.

The purpose of the monitor is to measure the amount of optical synchrotron radiation from the various FFTB magnets in the vicinity of IP1. We would like to observe the intensity, frequency dependence, and polarization. In principle we could also measure the position of the source of radiation, and the angular distribution. We present a design for a monitor that will measure the angular distribution of the radiation, with the option to measure the spatial profile by refocusing a lens.

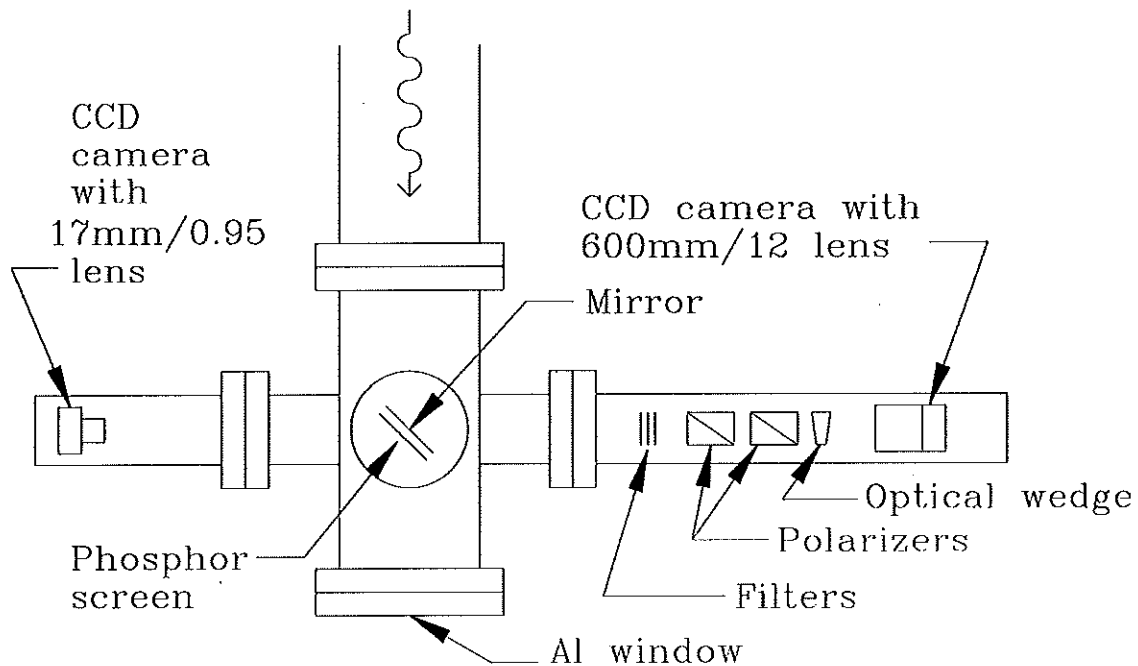


Figure 1: Top view of the synchrotron-radiation monitor.

The monitor is sketched in Fig. 1. Basically, a mirror reflects synchrotron-radiation by 90° into a CCD camera. A polarizing filter and/or prism can be placed in front of the camera lens.

Eventually Dave Meyerhofer's timing diagnostic will be located at IP1 (or perhaps IP2). At IP1 the synchrotron radiation from the soft bend magnet just upstream still overlaps the electron beam to some extent, and it will be difficult to extract the light without putting matter into the electron beam. Hence it may be best to locate the monitor downstream of the dump-magnet string. To implement a monitor this Summer it seems best to put it at the end of the γ -beam vacuum pipe, about 10 m downstream of IP2, as shown in Fig. 2.

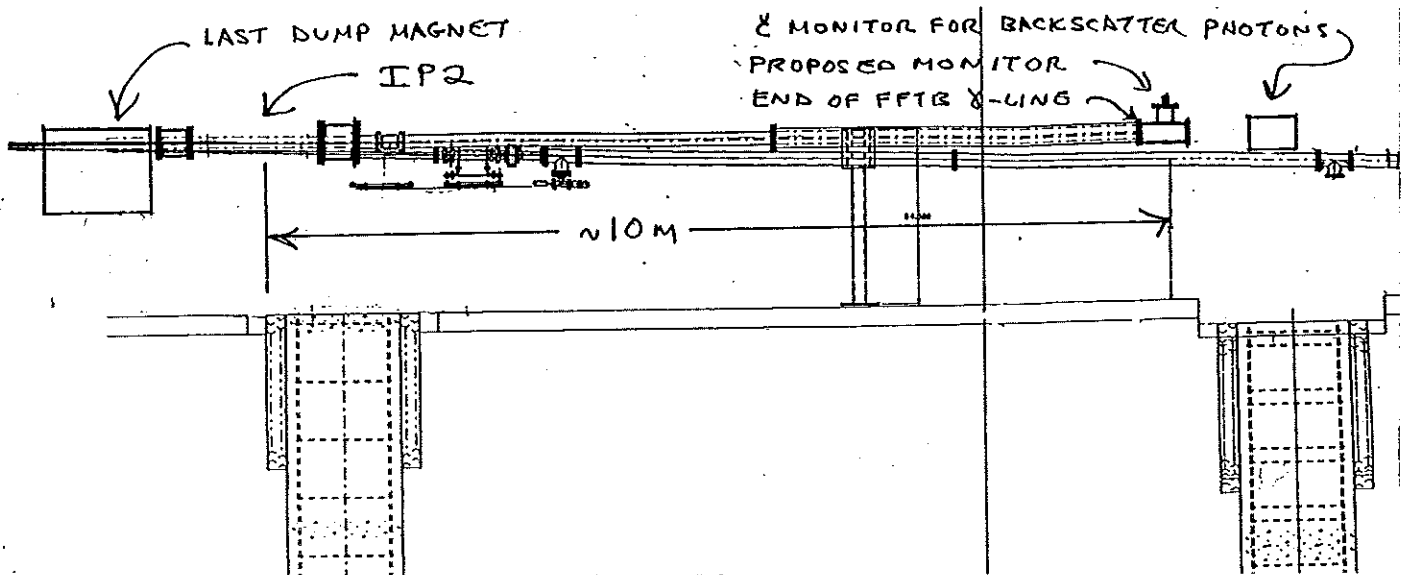


Figure 2: Side view of the FFTB γ -beam downstream of IP2, showing the proposed location of the synchrotron-radiation monitor.

We also propose to place one of Dieter Walz's aluminum-oxide phosphor screen on the back of the mirror to observe the profile of radiation in the MeV range. A second CCD camera will view this screen, as shown in Fig. 1.

2 Design of the Monitor

2.1 Goals

We propose to survey the optical synchrotron radiation produced in the four soft bend magnets surrounding IP1. The primary goal is to measure the intensity and frequency spectrum of the radiation. The polarization is readily observed by adding a polarizing filter. We would also like to determine the source(s) of the radiation. A goal of lesser importance is measurement of the spatial profile of the radiation, which largely depends on the profile of the electron beam. Finally, it will be relatively easy to add a monitor of the spatial profile of radiation in the MeV energy range.

2.2 General Optical Considerations

A desirable value for the aperture of the monitor is determined as follows. The total bend angle caused by the soft-bend magnets is about 1.1 mrad ($= 0.5 + 0.06 + 0.06 + 0.5$ mrad). In addition, we wish to survey the radiation produced in the FFTB quadrupoles near the final focus. In sec. 5 below we estimate that this radiation lies within 1 mrad of the beam axis (prior to deflection in the dump magnets. It appears reasonable to design the monitor to have angular coverage of ± 1.25 mrad. As the monitor is located about 20 m downstream of IP1, the aperture of the monitor must then be about 50 mm.

The design of the optics of the monitor is determined largely by details of the angular distribution of the synchrotron radiation. The deflection of the electron beam in the various dump magnets imparts a correlation between the point of emission of synchrotron radiation and the angle of emission, and hence the position of the radiation at the monitor. The synchrotron radiation intercepted by the monitor can be imaged in either of two ways. The spatial profile of the radiation (on any plane between the source and the monitor) can be imaged onto a sensor, or the angular distribution can be converted to a spatial distribution by placing the sensor in the focal plane of a lens. We now examine the merits of these two approaches.

The characteristic angular width of the radiation pattern from a localized region of the path of a single electron is $\approx 1/\gamma = 10 \mu\text{rad}$. Thus at the monitor 20 m downstream of IP1 the corresponding synchrotron-radiation spot has radius of only $200 \mu\text{m}$. However, at IP1 the electron beam has transverse size $\sigma_r \approx 1.5$ mm and divergence $\sigma_{r'} \approx 40 \mu\text{rad}$. This smears the radiation spot by $800 \mu\text{m}$ due to the angular divergence of the beam, and 1.5 mm by the spatial extent of the beam. Also, as discussed in sec. 3 below, diffraction due to the permanent-dump-magnet vacuum chamber smears the angular distribution by $17 \mu\text{rad}$ for $\lambda = 0.5 \mu\text{m}$. Hence the effective angular divergence of the synchrotron radiation is dominated by the divergence of the electron beam.

A direct measurement of the angle of the radiation will have an accuracy of at best about $40 \mu\text{rad}$, about 1 part in 60 of the 2.5-mrad angular acceptance of the monitor. If instead the spatial profile of the radiation is measured at the monitor, the spot size from a localized region along the electron beam will have $\sigma \approx 1.5$ mm, from which we infer the angle to emission to accuracy $(1.5 \text{ mm})/(20 \text{ m}) = 75 \mu\text{rad}$. If the spatial profile of a plane upstream of the monitor is measured (by imaging it onto the monitor) then the accuracy of measurement of the angle of emission is reduced. Of course, if the monitor images the radiation at the plane of, say, IP1 then almost no angular information is obtained, but rather we simply observe the spatial profile of the electron beam.

Hence it appears that the best information as to the source of the radiation can be obtained by a direct measurement of the angle of the radiation.

Table 1 summarizes the parameters discussed above that influence the design of the monitor.

2.3 CCD Camera

The task now is to measure the angular and spatial profiles of the synchrotron radiation at the monitor. We saw in the preceding subsection that the best achievable angular resolution

Table 1: Parameters of optical synchrotron radiation. The ‘Spot Size’ is measured at the monitor, taken to be 20 m downstream of IP1. The diffraction is due to the aperture of the vacuum chamber in the permanent dump magnets. The electron-beam parameters are taken from the standard FFTB beam tune according to Jim Spencer.

| Parameter | Value | Spot Size |
|--|--------------------|-------------------|
| Intrinsic angular spread = $1/\gamma$ | 10 μrad | 200 μm |
| Diffraction at $\lambda = 0.5 \mu\text{m}$ | 17 μrad | 333 μm |
| σ_r of electron beam at IP1 | 1.5 mm | 1.5 mm |
| $\sigma_{r'}$ of electron beam at IP1 | 40 μrad | 800 μm |
| Total angular acceptance $\Delta\theta$ of monitor | 2.5 mrad | 50 mm |
| No. of angular bins = $\Delta\theta/\sigma_{r'}$ | 63 | |

is about 1 part in 60, so the optical sensor need not have many more than 60 elements in each direction.

We propose to use an Electrim EDC-1000 CCD camera, which is also being used by the U. Rochester group for laser profile monitors. This camera has a TI-211 CCD with 192×165 pixels each $13.75 \mu\text{m} \times 16 \mu\text{m}$ for an active area of $2.64 \text{ mm} \times 2.64 \text{ mm}$. A frame can be read out in about 30 msec, so the camera could keep up with the 10-Hz rate of the FFTB, if desired.

2.4 Mirror

A 75-mm-diameter mirror deflects the optical synchrotron by 90° into the CCD camera. While more optical mirror use a glass substrate it may be wiser to use a metal substrate, to avoid possible cracking due to accumulation of stopping electrons. A candidate mirror is part A8010-301 from Janos Technology.

2.5 Lens

The (first) lens for the CCD camera must have a diameter D of at least 50 mm to subtend the desired 2.5 mrad. The most demanding specifications for the lens are set by the measurement of the angular distribution of the optical synchrotron radiation.

2.5.1 Measurement of the Angular Distribution

If the CCD is placed in the focal plane of this lens then light incident at angle θ to the optic axis is focused to position $\Delta x = f\theta$ on the CCD. The desired angular resolution is taken to be $\sigma_\theta = 40 \mu\text{rad}$, the angular divergence of the electron beam in the standard tune. To map one σ_θ onto one pixel of the CCD requires

$$f_{\min} = \frac{13.75 \mu\text{m}}{40 \mu\text{rad}} = 344 \text{ mm.}$$

The lens must, of course have aperture ratio f/D small enough that $D = 50 \text{ mm}$, *i.e.*, $f/D \leq 6.9$ for $f = 344 \text{ mm}$, *etc.*

The longest focal length of interest is such that the full desired angular acceptance of $\Delta\theta = 2.5 \text{ mrad}$ is mapped onto the whole 2.64-mm CCD. Hence

$$f_{\max} = \frac{2.64 \text{ mm}}{2.5 \text{ mrad}} = 1056 \text{ mm.}$$

Such a lens must have $f/D \leq 21$.

The lens must be color corrected over a reasonable range, say, 400-800 nm, and be capable of resolving 1 pixel (13.75 μm) in the center of its field. It may be advantageous to use a lens of focal length larger than 344 mm to blow up the image so the resolution of the lens is less of an issue.

It may be advantageous to use a lens that can be attached directly to the CCD camera, which has C-mount threads. Most commercial lenses made for cameras have C-mount adapters, so the choice of lens is broad. We are, however, thereby excluding lens made for enlargers, which may have superior optical properties (as well as typically higher cost). Table 2 lists several options for commercial camera lenses.

A reasonable choice may be the Canon FD 600/4.5 lens. The longer wavelength spreads the image of the 2.5-mrad acceptance over 1.5 mm of the CCD, and the are nearly two pixels per bin of 40 μrad . Canon lenses have somewhat lesser quality than Nikon or Leica, but we will only use the central 50 mm, corresponding to $f/D = 12$, and our angular field of view is only 2.5 mrad. (Indeed, we should set the f -stop to this value to insure better optical quality). If there is doubt about the Canon lens, perhaps the Leica R 500/8 is also a good choice.

The above scenario uses only a single lens of long focal length. It is possible to use two lenses: the first with a short focal length and a second that magnifies the image in the focal plane of the first lens. This solution is awkward in that two lens must be mounted and aligned, and that one can doubt that the first lens is capable of delivering the implied resolution of only a few microns at its focal plane.

2.5.2 Profile Measurement

In the measurement of the angular distribution of the optical synchrotron radiation the lens is focused at infinity. By focusing the lens near its minimum distance we can obtain a measurement of the spatial profile with the same apparatus.

To observe the spatial profile of the light at a plane with distance z from IP1 we simply consider this plane as the object O of the optical system, and the CCD the image I . We

Table 2: Survey of 35-mm camera lenses with focal length greater than 300 mm and apertures greater than 50 mm. We list lenses from Leica, Nikon and Canon as examples of the better quality. The prices are from a recent ad for B&H Camera, apparently the largest of the New York discount houses.

| Lens | f (mm) | f/D | D (mm) | Price |
|------------|-------------|-------|-------------|--------|
| Nikon A1-S | 300 | 4 | 75 | \$600 |
| Canon FD | 300 | 4 | 75 | \$520 |
| Nikon ED | 400 | 5.6 | 71 | \$1550 |
| Canon FD | 400 | 4.5 | 89 | \$1000 |
| Leica R | 500 | 8 | 63 | \$2500 |
| Nikon ED | 500 | 4 | 125 | \$3600 |
| Nikon ED | 600 | 5.6 | 107 | \$3500 |
| Canon FD | 600 | 4.5 | 133 | \$2650 |
| Nikon ED | 800 | 5.6 | 143 | \$4700 |

wish to image the profile corresponding to an angular region of 2.5 mrad onto the 2.64-mm CCD. Hence we need a demagnification of $(z \cdot 2.5 \text{ mrad})/2.64 \text{ mm}$ which is, of course, the ratio of distances O/I . The monitor lens is at $z = 20 \text{ m}$, so the object plane is at $z = 20 - O$. The lens formula then tells us

$$O = f(1 + O/I) = f(1 + 0.95(20 - O)), \quad \text{or} \quad O = \frac{20f}{1 + 0.95f},$$

for f and O in meters. Commercial lenses can typically focus only for $O \geq 10f$, which constraint will be satisfied by the previous equation for lenses of interest to us.

For example, if we use a lens with $f = 600 \text{ mm}$, then the profile of the synchrotron radiation would be measured at $O = 7.6 \text{ m}$ upstream of the monitor.

We could also focus the lens on IP1 to measure the profile of the light there, which will correspond closely to the profile of the electron beam with only slight vertical smearing due to the bend magnets.

2.6 Intensity

As an example, we consider the light from one of the 0.5-mrad soft bend magnets as observed by the angular distribution monitor.

In sec. 4 below we estimate that this magnet produces 10^7 optical photons per 10^{10} electrons. The angular spread of this radiation is over about 0.5-mrad vertically and $2 \times 40 = 80 \mu\text{rad}$ horizontally. An $f = 600$ mm lens will focus this light onto a region of $20 \times 4 = 80$ pixels of the CCD. Hence we expect about 1.25×10^5 photons/pixel, or perhaps 25,000 photoelectrons/pixel supposing the transmission factors times quantum efficiency is 20%.

The full-well signal of the Electrim CCD is about 100k electrons (and the stated signal-to-noise is quoted as 60 dB, which implies only 100-electron noise!). With an 8-bit ADC each count then corresponds to 400 electrons.

Hence the expected signal from the 0.5-mrad magnets should fall comfortably within the dynamic range of the CCD. The signal from the very soft bend magnets is larger by about a factor of 4 per pixel, so might be too large for the CCD. We estimate that the synchrotron radiation from the quadrupoles is of the same order as that in the bends but spread over an angular region perhaps 10 times larger, so this radiation should also be accessible to measurement.

Note that we cannot simply close the iris of the lens to reduce the intensity of light on the CCD, because the radiation from any particular electron does not fill the aperture. Rather we must use neutral density filters (or chromatic dispersion) to limit the intensity. Newport sells 2"-square filters, part FS-ND for a set, and filter holder FH-1.

The filters, along with the optical wedge and polarizing prisms discussed below will be mounted on an optical rail such as Oriel 11422 between the vacuum window and the CCD camera.

2.7 Spectral Analysis

We can place a prism upstream of the lens to disperse the light horizontally across the CCD, permitting spectral analysis of the optical synchrotron radiation. We can disperse the light horizontally from its angular spread of $40 \mu\text{rad}$ so that a specified wavelength interval covers the full 2.5-mrad acceptance of the monitor. If we use a lens with focal length 600 mm, then if the dispersion is performed just in front of the lens the total dispersion angle should be $\Delta\theta = 4$ mrad. The CCD camera is sensitive to roughly 400-1100 nm, which we take as the desired range for spectral analysis.

Since the desired dispersion angle is small we consider use of a 'wedge' prism of angle θ_{wedge} with the light normally incident on one face of the wedge. Then

$$\Delta\theta = \Delta n \theta_{\text{wedge}},$$

where Δn is the difference between the indices of refraction at 400 and 1100 nm. For example, with BK7 glass the wedge angle should be 9° to yield 4-mrad dispersion, or 11° for fused silica.

The only 50-mm-diameter wedges (of angles larger than 3° and less than 45°) are available as a semi-custom order from Janos Technology.

The 9° wedge will cause a 4° average deflection of the light. Therefore the CCD camera must be mounted on an arm that can rotate about the center of the wedge.

2.8 Polarization Analysis

Dave Meyerhofer's timing diagnostic works best for polarized light. Synchrotron radiation from the vertical bend magnets should be about 90% polarized with **E** vertical. However, the synchrotron radiation from the quads will have approximately zero net polarization, as the electrons are deflected both horizontally and vertically by similar amounts.

In principle we wish to study the optical synchrotron radiation over the 50-mm aperture of the monitor, and over the full spectral sensitivity of the CCD (≈ 400 -1100 nm). However, the largest good quality polarizer appears to be 38-mm cubes from Melle Griot, 03 PBB 007 for 450-700 nm, and 03 PBB 017 for 650-850 nm. We could use the two cube together to cover the range 450-850 nm.

We will need filters to limit the bandwidth to that over which the polarizers work well. This could be done with a Corion LL-450-S long-wave-pass filter and a LS-850-S short-wave-pass filter, both 50 mm square.

2.9 Monitor of MeV Radiation

If we put a phosphor screen on the back side of the 45° mirror then we can also observe the spatial distribution of electrons emerging from the mirror. Only photons of energies above a few MeV have significant probability of producing any such electrons. Ideally there should be very few of these higher-energy photons.

The mirror will have an effective thickness of about 20% of a radiation length. We might want to place 1-2 cm of lead between the mirror and the phosphor screen to increase the number of electrons in the beam.

We will use a second Electrim EDC-1000 CCD camera to view the phosphor screen. The demagnification should be $I/O = (2.64 \text{ mm})/(50 \text{ mm}) = 1/19$. If a lens with focal length $f = 17 \text{ mm}$ is used, the object distance should be $O = f(1 + O/I) = 340 \text{ mm}$. This is just outside the vacuum window of the monitor.

The depth of field is not good for such a short object distance. If the object distance changes by amount δO then the image of a point source is spread over a distance

$$\delta x = \frac{\delta O}{f/D} \left(\frac{I}{O}\right)^2$$

on the nominal image plane. For the phosphor screen we have δ) up to 25 mm, so δx is as large as $(70 \mu\text{m})/(f/D)$.

We could use a lens with $f/D = 0.95$ (\$600 from JML) to maximize the light collection. But then the image from a point at the edge of the phosphor screen would be spread over 5 pixels on the CCD. However, since the electron beam has $\sigma_r \approx 1.5 \text{ mm}$, the minimum spot size on the phosphor screen will be about the same value, which translates to 80 μm on the CCD. Hence the depth of field of even an $f/D = 0.95$ lens is matched to the intrinsic resolution of the monitor.

2.10 Vacuum Vessel

The mirror (and phosphor screen) are the only elements of the monitor that are inside the FFTB vacuum pipe. The mirror is inside a 5-way cross consisting of a 6"-diameter pipe

extension of the existing vacuum pipe, plus three transverse penetration to let the light out and to support a motion feedthrough from which the mirror is hung.

The 45° mirror has diameter of 3" so that it intercepts a 50-mm beam. Hence the vertical penetration for the motion feedthrough should have 4" diameter. The motion feedthrough will be an MDC model HLM with 3" travel and pneumatic actuation. We will construct a simple spring-loaded pin mechanism to align the mirror when it is moved into the beam.

The horizontal penetrations are only to let the light out, and so could be as narrow as 2" in diameter. Perhaps it is wiser to make them 3" in diameter so that misalignments could still be corrected.

The vacuum windows will be of ordinary glass, MDC part 450005.

2.11 Cost Estimate

| | |
|---|----------|
| 1. Custom 5-way cross (MDC) | \$1500 |
| 2. 2 vacuum windows on CF4-5/8 (MDC 450005) | \$500 |
| 3. 3" travel motion feedthrough on CF6 (MDC HLM series) | \$900 |
| 4. 3"-diameter Al mirror (Janos A8010-301) | \$225 |
| 5. 2 CCD cameras (Electrim EDC-1000) | \$800 |
| 6. Canon FD 600mm/4.5 lens | \$2700 |
| 7. 17mm/0.95 CCTV lens (JML) | \$600 |
| 8. 2"-square neutral density filter set (Newport FS-ND) | \$1000 |
| 9. Bandpass filter set (Corion LL-450-S, LS-850-S) | \$300 |
| 10. Polarizing prisms (Melle Griot 03 PBB 007 and 03 PBB 017) | \$700 |
| 11. 9°, 2"-diameter optical wedge (Janos) | \$500 |
| 12. 12" optical rail (Oriol 11422) | \$250 |
| 13. 4 rail carriers (Oriol 11641) | \$300 |
| 14. Filter holder (up to 38 mm thick) (Newport FH-1-B3) | \$100 |
| 15. 2 prism holders (Oriol 12680) | \$200 |
| 16. Chuck for optical wedge (Newport AC2-B3) | \$150 |
| 17. 486 PC | \$2500 |
| 18. Total | \$13,225 |

The camera support plates and stand for the monitor will be constructed at Princeton at no direct cost other than materials.

3 Diffraction of Optical Synchrotron Radiation

The angular distribution of synchrotron radiation has characteristic angular width $1/\gamma = 10 \mu\text{rad}$ for 50-GeV electrons. This is a remarkably narrow angular distribution when one considers optical frequencies. Indeed, the usual lore (*i.e.*, Heisenberg's uncertainty principle, laws of diffraction, *etc.*) is that a beam of light of angular divergence $\theta = 1/\gamma$ can only emerge from a source of transverse aperture $D \gtrsim \lambda\gamma$. If we take $\lambda = 0.5 \mu\text{m}$ as an example, then we would expect the source size must be $D \gtrsim 5 \text{ cm}$. But synchrotron radiation results from even a single electron, whose transverse size is $\lambda_C \approx 10^{-11} \text{ cm}$.

We believe there is no contradiction here, and the synchrotron radiation maintains its angular spread of $\approx 1/\gamma$ so long as the radiation propagates in vacuum. Consider the instantaneous rest frame of the electron. In this frame there is no problem with diffraction; the radiation pattern is that of a dipole, and spreads out in all directions. In the lab frame we observe the Lorentz transformation of this dipole angular distribution, and the lab-frame angular distribution narrows to $\approx 1/\gamma$.

The laws of diffraction remain in effect in the following sense. The wavefronts of some wavelength λ must have a particular amplitude and phase dependence over transverse dimensions $\gtrsim \gamma\lambda$ that conspires to yield angular divergence of only $1/\gamma$. As a consequence, if the synchrotron radiation is observed through an aperture of radius r (such as a beampipe) the loss of the large-radius component of the wavefront will result in a broadening of the angular distribution. Roughly, we expect $\theta \gtrsim r/\lambda$.

In the FFTB, the vacuum box of the permanent dump magnets limits the horizontal aperture to about 3 cm. For our monitor downstream of these magnets the angular distribution of $\lambda = 0.5 \mu\text{m}$ radiation will then be broadened to about $17 \mu\text{rad}$, or $5/3$ times the intrinsic width. Hence the horizontal spot size of optical radiation from a single electron observed at our monitor some 20 m downstream will be $\approx \pm 333 \mu\text{m}$. I don't know what is the limiting vertical aperture, but it may well be larger than 3 cm, so vertical diffraction would be less.

Of course, if the synchrotron radiation is intercepted by a mirror, lens or window of aperture smaller than the beampipe, further diffraction of the angular distribution will occur.

4 Synchrotron Radiation During Cyclical Motion

The radiation of charged particles executing large numbers of cycles of circular motion was first studied by Schott [1], but became well known only with the works of Arzimovitch and Pomeranchuk [2] and Schwinger [3]. In this note we start from the review by Sands [4], but convert the formulae to ones involving the QED critical field strength

$$B_{\text{crit}} = \frac{m^2 c^3}{e\hbar} = 4.41 \times 10^{13} \text{ Gauss.}$$

The total radiation rate follows directly from the Larmor formula and is given by Sands' eq. (4.4) as for the case of motion involving many complete cycles in a circular storage ring:

$$P_\gamma = \frac{2}{3} \frac{e^2 a^{\prime 2}}{c^3} = \frac{2}{3} \alpha \frac{c}{\lambda_C} m c^2 \left(\frac{\gamma B}{B_{\text{crit}}} \right)^2.$$

The photon-number spectrum $n(u)$ per second per unit energy u is given by Sands' eq. (5.8) as

$$n(u)du = \frac{P\gamma}{u_c^2} F(u/u_c)du,$$

where the so-called critical energy is given by Sands' eq. (5.9) as

$$u_c = \frac{3}{2} mc^2 \frac{\gamma^2 B}{B_{\text{crit}}}.$$

For the case of interest, the infrared-photon energy u is small compared to the critical energy, so we combine Sands' eqs. (5.6) and (5.10) to find

$$F(u/u_c) \approx 1.34(u_c/u)^{2/3}, \quad (u \ll u_c),$$

and hence

$$n(u)du \approx 0.4\alpha \frac{c}{\lambda_C} \frac{1}{\gamma^2 mc^2} \left(\frac{u_c}{u}\right)^{2/3} du.$$

I prefer to convert this rate per second into a rate over path length L in the magnetic field, and to insert the expression for u_c in terms of magnetic field. This leads to

$$n(u)du \approx 0.5\alpha \frac{L}{\lambda_C} \frac{1}{\gamma^{2/3}(mc^2)^{1/3}} \left(\frac{B}{B_{\text{crit}}}\right)^{2/3} \frac{du}{u^{2/3}} \approx 0.001 \frac{LB^{2/3}}{\gamma^{2/3} u^{2/3}},$$

for path length L in cm, magnetic field B in Gauss, and photon energy u in eV. Then for a 50-GeV electron, $\gamma^{2/3} \approx 2000$, so

$$n(u)du \approx 5 \times 10^{-7} LB^{2/3} \frac{du}{u^{2/3}}.$$

The very soft bend magnet just upstream of IP1 has $L = 100$ cm and $B = 100$ Gauss. Then we expect

$$n(u)du \approx 10^{-3} \frac{du}{u^{2/3}}.$$

For $du/u^{2/3} = 1$ at $u = 1$ eV, and a beam of 10^{10} electrons we then have 10^7 synchrotron-radiation photons.

The soft bend magnets with $L = 100$ cm and $B = 667$ Gauss yield about 4 times as many infrared photons.

When discussing the amount of radiation collected in an optical system it is useful to display the radiation rate as a function of bend angle in the magnets. If the magnet has length L and field B then the bend angle is

$$\theta = \frac{1}{\gamma} \frac{L}{\lambda_C} \frac{B}{B_{\text{crit}}},$$

and the photon-number spectrum per radian is

$$n_\theta(u)du \approx 0.5\alpha \left(\frac{\gamma B_{\text{crit}}}{mc^2 B}\right)^{1/3} \frac{du}{u^{2/3}}.$$

For 50-GeV electrons this becomes

$$n_\theta(u)du \approx \frac{70}{B^{1/3}} \frac{du}{u^{2/3}}.$$

Note that per unit deflection angle, a weaker magnet produces more optical radiation than a strong one!

In the very soft bend magnet with $L = 100$ cm and $B = 100$ Gauss the bend angle is 58 μ rad, and we arrive at the same estimate for the radiation rate as given previously.

5 Synchrotron Radiation in Quadrupoles

There may be significant synchrotron radiation in the FFTB quadrupoles upstream of IP1. Here we make a simple rate estimate. Jim Spencer is working on a more detailed calculation via ray tracing.

Since the field of a quadrupole varies linearly with distance from the beam axis, synchrotron radiation is prominent only for off-axis electrons. Typically the beam is wider in one projection than the other, so we estimate only for the wider projection, calling it x . We also ignore variation in x for an electron when in the quadrupole field. Then we simply characterize the beam profile as a gaussian with variance σ_x . The field, of course, can be written as $B(x) = Kx$.

From the previous section we know that the number of synchrotron radiation photons emitted per unit length will vary as $B^{2/3}$. Hence the radiation rate integrated over the beam profile depends on the quadrupole gradient K as

$$\frac{\sqrt{2}}{\sigma_x \sqrt{\pi}} \int_0^\infty e^{-x^2/2\sigma_x^2} B^{2/3} dx \approx (0.7K\sigma_x)^{2/3}.$$

That is, the quadrupole has an effective field strength $B \approx 0.7K\sigma_x$ so far as synchrotron radiation is concerned.

For the FFTB, the largest σ_x or σ_y are about 2.5 mm, according to Jim Spencer's presentation at the February E-144 group meeting (p. 61 of the Proceedings). Jim informs us that for the magnets in question $K = (9.55 \text{ kG})/(26 \text{ mm})$, and their length is 2 m. The effective field strength for synchrotron radiation is then about 640 Gauss. Hence we expect that the quads where the beam is the largest cause about the same amount of synchrotron radiation as the 0.5-mrad soft-bend magnets.

The angular divergence of the beam at the final focus is $\sigma_{x'} = 0.3$ mrad, and $\sigma_{y'} = 0.6$ mrad. As the beam passes through the quadrupoles the beam divergence will vary by perhaps as much as a factor of 2. Hence we infer that the synchrotron radiation from the quadrupoles will occur mainly at angles 0.5-1 mrad from the beam axis.

6 Synchrotron Radiation in a 'Short' Magnet

Details of the soft end of the synchrotron-radiation spectrum have not been as well studied as at the hard end. As noted in Appendix B of the E-144 proposal, the radiation spectrum

due to a small kick in a single ‘short’ magnet is not necessarily the same as that due to a ‘long’ magnet.

This effect was first discussed by Coisson’s [5, 6] who noted that the standard results for the spectrum of synchrotron radiation hold only if the particle is deflected by an angle larger than the characteristic width of the angular distribution of the radiation, namely $1/\gamma$. For 50-GeV electrons this angle is $10 \mu\text{rad}$, so even the very soft bends (that cause a $58\text{-}\mu\text{rad}$ deflection) are ‘long’ magnets. The very soft bend magnets would be ‘short’ if their fields were reduced to $\lesssim 16$ Gauss.

Coisson also noted that if the magnetic field strength changes significantly over a distance corresponding to a deflection angle less than $1/\gamma$, then the radiation spectrum is distorted from that due to an adiabatic approximation. In general, the spectrum in a rapidly varying field is wider than that due to a uniform field, with enhancements at both high and low frequencies. The enhancement at high frequencies has been verified by measurement of optical synchrotron radiation from protons at CERN [7, 8].

At the FFTB the fields in the dump magnets fall off in less than 5 cm, corresponding to ‘edge’ deflections less than 5% of that in the full 100-cm magnets. Only for the very soft bend magnets is edge deflection ($\lesssim 3 \mu\text{rad}$) less than $1/\gamma$. It would be interesting to look for a distortion of the radiation spectrum due to the two edges of the very soft bend magnets surrounding IP1. However, to see this effect the angular resolution of the optical system must be $\sim 1 \mu\text{rad}$, and the angular divergence of the electron beam must be of this order also.

Synchrotron radiation in ‘short’ magnets is discussed further in papers by Bagrov *et al.* [9, 10], and by Hoffman and Méot [11]. A paper by Pomeranchuk [12] written in 1939 deserves notice. In this the earth is considered as a ‘short’ magnet that leads to large radiation from cosmic ray electrons. Indeed, Pomeranchuk notes that for electrons of energy greater than 10^{19} eV the earth’s field appears to exceed the QED critical field strength and pair production is likely.

7 Interference of Synchrotron Radiation

Nikitin *et al.* [13] have observed an interesting interference effect in synchrotron radiation from the ends of two magnets separated by a straight section of length L . Interference is prominent if the time delay between electrons and photons crossing the straight section is roughly one cycle. That is

$$\frac{\lambda}{c} \approx \Delta t = \frac{L}{\beta c} - \frac{L}{c} \approx \frac{L}{2\gamma^2 c}.$$

The interference can therefore be observed at wavelengths

$$\lambda \approx \frac{L}{\gamma^2}.$$

For 50-GeV electrons the 1-m straight section at IP1 leads to interference effects for $\lambda \approx 10^{-4} \mu\text{m}$, *i.e.*, for photon energies of about 10 KeV (which happens to be about the critical energy in the very soft bend magnets).

Hence this interference effect will not be important in our measurement of optical synchrotron radiation.

8 Coherence Effects

For wavelengths longer than the typical spacing between electrons in the beam bunch, coherence effects may be important.

For example, a nominal FFTB bunch has 10^{10} electrons, a radius of 1 mm (when passing through the dump magnets), and length of 3 ps = 1 mm. In this case the average spacing is $0.5 \mu\text{m}$, just the wavelength of visible light. But if the spot were focused to, say, a radius of 0.1 mm then the average spacing would be only $0.1 \mu\text{m}$, for which coherence effects might be noticeable.

The question remains as to what the coherence effect might be. In the first approximation there may be little effect, following the argument of sec. 20-4 (see also sec. 22-4) of Panofsky and Phillips [14] that in the presence of random density fluctuations the intensity of the radiation remains directly proportional to the number of charges.

9 References

- [1] G.A. Schott, *Electromagnetic Radiation*, (Cambridge University Press, 1912).
- [2] L. Arzimovitch and I. Pomeranchuk, *The Radiation of Fast Electrons in the Magnetic Field*, J. Phys. (Sov.) **9** (1945) 257.
- [3] J. Schwinger, *On the Classical Radiation of Accelerated Electrons*, Phys. Rev. **75** (1949) 1912.
- [4] M. Sands, *The Physics of Electron Storage Rings*, SLAC-121 (1970).
- [5] R. Coisson, *On Synchrotron Radiation in Nonuniform Magnetic Fields*, Opt. Comm. **22** (1977) 135.
- [6] R. Coisson, *Angular-Spectral Distribution and Polarization of Synchrotron Radiation from a "Short" Magnet*, Phys. Rev. A **20** (1979) 524.
- [7] R. Bossart *et al.*, *Observation of Visible Synchrotron Radiation Emitted by a High-Energy Proton Beam at the Edge of a Magnetic Field*, Nucl. Instr. and Meth. **164** (1979) 375.
- [8] R. Bossart *et al.*, *Proton Beam Profile Measurements with Synchrotron Light*, Nucl. Instr. and Meth. **184** (1981) 349.
- [9] V.G. Bagrov *et al.*, *Charged Particle Radiation in Magnetic Systems*, Nucl. Instr. and Meth. **195** (1982) 569.
- [10] V.G. Bagrov *et al.*, *Radiation of Relativistic Electrons Moving in an Arc of a Circle*, Phys. Rev. D **28** (1983) 2464.
- [11] A. Hoffmann and F. Méot, *Optical Resolution of Beam Cross-Section Measurement by Means of Synchrotron Radiation*, Nucl. Instr. and Meth. **203** (1982) 483.

- [12] I. Pomeranchuk, *On the Maximum Energy Which the Primary Electrons of Cosmic Rays Can Have on the Earth's Surface Due to Radiation in the Earth's Magnetic Field*, J. Phys. (Sov.) 2 (1940) 65.
- [13] M.M. Nikitin *et al.*, *Interference of Synchrotron Radiation*, Sov. Phys. JETP 52 (1980) 388.
- [14] W.K.H. Panofsky and M. Phillips, *Classical Electricity and Magnetism*, 2nd ed. (Addison-Wesley, Reading, MA, 1962).